Thermodynamic Evidence for Ca²⁺-Mediated Self-Aggregation of Lewis X Gold Glyconanoparticles. A Model for Cell Adhesion via Carbohydrate−Carbohydrate Interaction

Jesús M. de la Fuente,[†] Peter Eaton,[†,§] Africa G. Barrientos,[†]
Margarita Menéndez,[‡] and Soledad Penadés*,[†]

Contribution from Grupo de Carbohidratos, Laboratory of Glyconanotechnology, IIQ/CSIC, Americo Vespucio 49, 41092 Seville, Spain, and Departamento Química-Física de Macromoléculas Biológicas, IQFR/CSIC, Serrano 119, 28006 Madrid, Spain

Received November 15, 2004; E-mail: penades@iiq.csic.es

Abstract: Thermodynamic evidence for the selective Ca²⁺-mediated self-aggregation via carbohydrate−carbohydrate interactions of gold glyconanoparticles functionalized with the disaccharides lactose (*lacto*-Au) and maltose (*malto*-Au), or the biologically relevant trisaccharide Lewis X (Leˣ−Au), was obtained by isothermal titration calorimetry. The aggregation process was also directly visualized by atomic force microscopy. It was shown in the case of the trisaccharide Lewis X that the Ca²⁺-mediated aggregation is a slow process that takes place with a decrease in enthalpy of 160 ± 30 kcal mol⁻¹, while the heat evolved in the case of lactose and maltose glyconanoparticles was very low and thermal equilibrium was quickly achieved. Measurements in the presence of Mg²⁺ and Na⁺ cations confirm the selectivity for Ca²⁺ of Leˣ−Au glyconanoparticles. The relevance of this result to cell−cell adhesion process mediated by carbohydrate−carbohydrate interactions is discussed.

Introduction

Cells use multiple mechanisms to bind to extracellular matrixes and to other cells.[1] Adhesion and recognition are important events in migration, differentiation, self-assembly, and communication of cells. Protein−protein interactions constitute an important mechanism for cell adhesion that controls cellular behavior.[1b] Because most cell surface proteins are highly glycosylated (glycoproteins), carbohydrate−protein interactions are also involved in cell adhesion and recognition.[2] Glycoproteins and glycolipids together with extracellular glycans create a dense coating around the cell called the glycocalyx,[3] potentially involved in repulsive functions. However, glycoproteins and glycolipids are ligands for toxins, bacteria, viruses, and other cells through carbohydrate−protein interactions.[4] In addition, interactions between carbohydrates are emerging as a versatile mechanism for cell adhesion and recognition.[5] Carbohydrate−

carbohydrate interactions between cell surface glycolipids mediate cell adhesion during embryogenesis, metastasis, and signal transduction.[6] Most of the structures involved in this novel mechanism are glycosphingolipids (GSL) organized in the plasma membrane as microdomains separated from the glyco-protein clusters.[7]

Characteristic features of carbohydrate−carbohydrate interactions are a strong dependency on divalent cations (Ca²⁺), a variable specificity, and an extremely low affinity that is compensated in nature by a multivalent presentation of the carbohydrate ligands at the cell surface. These features make the process difficult to study and quantify with monovalent ligands. As in the study of other biological interactions, the use of model systems has been a productive approach to understanding carbohydrate interactions. Qualitative studies on carbohydrate−carbohydrate interactions with model systems, although limited, span from simple monovalent to polyvalent systems and even whole cells.[5d] The first thermodynamic data on carbohydrate−carbohydrate interactions in water were obtained with a model system that consisted of a new type of synthetic receptor named glycophanes and a series of 4-nitro-

† IIQ/CSIC.

‡ IQFR/CSIC.

§ Current address: REQUIMTE, Departamento de Química, Faculdade de Ciências da Universidade do Porto, Rua do Campo Alegre, 687, 4169-007 Porto, Portugal.

(1) (a) Bell, G. I. *Science* **1978**, *200*, 618−627. (b) Rouslahti, E.; Pierschbacher, M. D. *Science* **1987**, *238*, 491−497. (c) Chothia, C.; Jones, E. Y. *Annu. Rev. Biochem.* **1997**, *66*, 823−862. (d) Gumbiner, B. M. *Cell* **1996**, *84*, 345−357. (e) Rustom, A.; Saffrich, R.; Markovic, I.; Walther, P.; Gerdes, H.-H. *Science* **2004**, *303*, 1007−1010.

(2) (a) Hakomori, S. *Proc. Natl. Acad. Sci. U.S.A.* **2002**, *99*, 225−232. (b) Brewer, C. F.; Miceli, M. C.; Baum, L. G. *Curr. Opin. Struct. Biol.* **2002**, *12*, 616−623.

(3) Frey, A.; Giannasca, K. T.; Weltzin, R.; Giannasca, P. J.; Reggio, H.; Lencer, W. I.; Neutra, M. R. *J. Exp. Med.* **1996**, *184*, 1045−1059.

(4) *Carbohydrates in Chemistry and Biology, Part II: Biology of Saccharides*; Ernst, B., Hart, G. W., Sinay, P., Eds.; Wiley−VCH: New York, 2000; Vol. 4.

(5) (a) Hakomori, S.-I. *Pure Appl. Chem.* **1991**, *63*, 473−482. (b) Spillman, D.; Burger, M. M. Carbohydrate−carbohydrate interactions. In *Carbohydrates in chemistry and biology*; Ernst, B., Hart, G. W., Sinay, P., Eds.; Wiley−VCH: Weinheim, 2000; Vol. 2, pp 1061−1091. (c) Bovin, N. H. Carbohydrate−carbohydrate interactions. In *Glycoscience: status and perspectives*; Gabius, H. J., Gabius, S., Eds.; Chapman & Hall: Weinheim, 1997; pp 277−289. (d) Rojo, J.; Morales, J. C.; Penadés, S. *Top. Curr. Chem.* **2002**, *218*, 45−92.

(6) Several authors. Glycosphingolipids and membrane domains. Sonnino, S., Tettamanti, G., Eds.; Kluwer Academic Publishers: Norwell, MA; *Glycoconjugate J.* **2000**, *17*, Nos. 3−4.

(7) Hakomori, S.-I. *Glycoconjugate J.* **2000**, *17*, 627−647.

phenyl glycosides.[8] Some additional quantitative data on carbohydrate−carbohydrate interactions have recently been reported.[9]

To further investigate carbohydrate−carbohydrate interaction with epitopes specifically involved in biological interactions, we have developed an integrated strategy that includes polyvalent model systems as well as analytical techniques to evaluate this interaction.[10] These model systems are based on self-assembled monolayers (SAMs) of neoglycoconjugates of biologically significance attached to two- (2D) or three-dimensional (3D) gold surfaces creating a polyvalent presentation of carbohydrate molecules.[10a] The 3D polyvalent system is based on sugar protected gold nanoclusters. With well-defined chemical composition and globular shape, the so-called glyconanoparticles (GNPs)[10b] provide a glycocalyx-like surface mimicking GSL patches at the cell surface. Following this strategy, we determined, by means of atomic force microscopy (AFM)[10c] and surface plasmon resonance (SPR),[10b] the adhesion forces and the kinetics of the self-recognition of the antigen Lewis X (Le^X, Galβ1-4[Fucα1-3]GlcNAcβ1). Auto-aggregation of F9 teratocarcinoma cells in the presence of Ca²⁺, mimicking the embryonal compaction process, was shown to be due to homotopic Le^X−Le^X interactions.[11] Water-soluble GNPs functionalized with the antigen Lewis X represent a good model to mimic the auto-aggregation of F9 carcinoma cells and morula compaction via carbohydrate−carbohydrate interaction.

The first data on self-aggregation of Le^X functionalized GNPs were obtained by mean of transmission electron microscopy (TEM).[10b] TEM micrographs of these GNPs dissolved in 10 mM calcium chloride solution showed 3D aggregates, the sizes of which depended on the concentration of GNPs. In contrast, control GNPs presenting the disaccharide lactose did not aggregate in the presence of calcium ions. The self-aggregation of the Le^X GNPs was calcium dependent, and addition of EDTA resulted in dispersion of the aggregates. It was argued that the aggregation events as observed on a carbon grid might be rather different from those of biological systems in physiological conditions.

To further demonstrate the selective Ca²⁺-mediated self-aggregation in solution of GNPs presenting the Le^X antigen, we now report the first thermodynamic data of this aggregation obtained by isothermal titration calorimetry (ITC) in aqueous solution and visualize this process by means of AFM. As control systems, we have also studied the aggregation of GNPs presenting the disaccharides lactose (*lacto*, Galβ1-4Glc) or maltose (*malto*, Glcα1-4Glc). The results now presented: (a) corroborate the aggregation of the Le^X glyconanoparticles in aqueous solution; (b) provide, for the first time, a thermodynamic estimation for the Ca²⁺-mediated self-aggregation of the Le^X antigen; and (c) confirm the Ca²⁺ selectivity of this association.

Experimental Section

Materials. Neoglycoconjugates **1**, **2**, and **3** were prepared as previously reported.[10a,12] The neoglycoconjugates were isolated as disulfide derivatives and in this form used to prepare the corresponding glyconanoparticles, Le^X−Au, *lacto*-Au, and *malto*-Au.[10a]

ITC Experiments. The calorimetric measurements were performed with a Microcal MCS-ITC at 25 °C. In a typical run, aliquots of an aqueous solution of the glyconanoparticles Le^X−Au, *lacto*-Au, and *malto*-Au were added into the calorimetric cell (operating volume 1.35 mL) with a 10 mM CaCl₂, MgCl₂, or NaCl solution in MilliQ water. The aqueous solution of GNPs was loaded into the injection syringe at 25−50 μM. All of the experiments were performed at 25 °C with data points taken every 2 s. For Le^X−Au experiments, typically three injections of 15 μL were made at 4000 s intervals after a first 1 μL injection. In *lacto*-Au or *malto*-Au experiments, 15 μL injections of the GNP solution were added into the calorimetric cell every 380 s after a first injection of 1 μL. The total heat evolved for each injection was corrected for the heat of dilution of the GNPs in water. The apparent enthalpy of association was estimated as the heat evolved per mole of GNP injected using the ITC-Origin software provided by Microcal Inc.:

$$\Delta H_{app} = -Q/([M] \cdot v)$$

where Q (μcal) is the experimental heat of injection after subtracting the heat of dilution, M is the glyconanoparticle concentration in the syringe (25 or 50 μM), and v is the injected volume (15 μL). The maximum number of injections per run for Le^X−Au was three due to the slowness of Le^X−Au association and the limits imposed by the size of the experimental-data collecting files.

AFM Experiments. AFM measurements were made with a Topometrix explorer AFM (Veeco Instruments, Sunnyvale, USA) in noncontact mode in air. The noncontact mode[13] was used to avoid any compression of the sample that may have occurred with contact mode AFM. Rectangular silicon cantilevers with integrated tips of spring constant 4.5 N/m (MikroMasch, Tallinn, Estonia) were used, oscillating at just below their natural resonant frequency (nominally 150 kHz, but measured for each cantilever) throughout the work. The radius of curvature of the tips was specified as less than 10 nm, but given the very small radius of the glyconanoparticles, significant image dilation is likely to have occurred.[14] Therefore, particle heights rather than lateral dimensions were used to characterize particle diameter. This has been shown to be the best method of measuring small particle diameters.[15,16] In the case of pure gold nanoparticles, it has been found that AFM height measurements and TEM measured diameters match closely.[16] Untreated gold glyconanoparticles were prepared for imaging by dissolving in pure water (18 MΩ, Sigma-Aldrich, UK), followed by centrifugation at 10 000g for 60 s to remove undissolved impurities. GNPs were deposited onto freshly cleaved mica from dilute (0.2 μM) solution, and left to air-dry. Ca²⁺, Mg²⁺, and Na⁺ treatment was carried out by incubating the GNPs in 10 mM CaCl₂, MgCl₂, or NaCl solutions for 24 h. The solution was filtered by centrifugation through a

(8) (a) Coteron, J. M.; Vicent, C.; Bosso, C.; Penadés, S. *J. Am. Chem. Soc.* **1993**, *115*, 10066−10007. (b) Jimenez-Barbero, J.; Junquera, E.; Martin-Pastor, M.; Sharma, S.; Vicent, C.; Penadés, S. *J. Am. Chem. Soc.* **1995**, *117*, 11198−11204. (c) Morales, J. C.; Zurita, D.; Penadés, S. *J. Org. Chem.* **1998**, *63*, 9212−9222.

(9) (a) Dammer, U.; Popescu, O.; Wagner, P.; Anselmetti, D.; Güntherodt, H.-J.; Misevic, G. N. *Science* **1995**, *267*, 1173−1175. (b) Matsuura, K.; Kitakuoji, H.; Sawada, N.; Ishida, H.; Kiso, M.; Kitajima, K.; Kobajashi, K. *J. Am. Chem. Soc.* **2000**, *122*, 7406−740. (c) Pincet, F.; Le Bouar, T.; Zhang, Y.; Esnault, J.; Mallet, J. M.; Perez, E.; Sinaÿ, P. *Biophys. J.* **2001**, *80*, 1354−1358. (d) Haseley, S. R.; Vermeer, H. J.; Kamerling, J. P.; Vliegenthart, J. F. K. *Proc. Natl. Acad. Sci. U.S.A.* **2001**, *96*, 9419−9424.

(10) (a) Barrientos, A. G.; de la Fuente, J. M.; Rojas, T. C.; Fernandez, A.; Penadés, S. *Chem.-Eur. J.* **2003**, *9*, 1909−1921. (b) de la Fuente, J. M.; Barrientos, A. G.; Rojas, T. C.; Rojo, J.; Canada, J.; Fernández, A.; Penadés, S. *Angew. Chem., Int. Ed.* **2001**, *40*, 2257−2261. (c) Tromas, C.; Rojo, J.; de la Fuente, J. M.; Barrientos, A. G.; Garcia, R.; Penadés, S. *Angew. Chem., Int. Ed.* **2001**, *40*, 3052−3055. (d) Hernaiz, M. J.; de la Fuente, J. M.; Barrientos, A. G.; Penadés, S. *Angew. Chem., Int. Ed.* **2002**, *41*, 1554−1557. (e) de la Fuente, J. M.; Penadés, S. *Glycoconjugate J.* **2004**, *21*, 149−163.

(11) Eggens, I.; Fenderson, B. A.; Toyokuni, T.; Dean, B.; Stroud, M. R.; Hakomori, S. *J. Biol. Chem.* **1989**, *264*, 9476−9484.

(12) de la Fuente, J. M.; Penadés, S. *Tetrahedron: Asymmetry* **2002**, *13*, 1879−1888.

(13) Hofer, W.; Foster, A. S.; Shluger, A. L. *Rev. Mod. Phys.* **2003**, *75*, 1287.

(14) Gibson, C. T.; Watson, G. S.; Myhra, S. *Scanning* **1997**, *19*, 564−581.

(15) Sato, H.; Ohtsu, T.; Komasawa, I. *J. Colloid Interface Sci.* **2000**, *230*, 200−204.

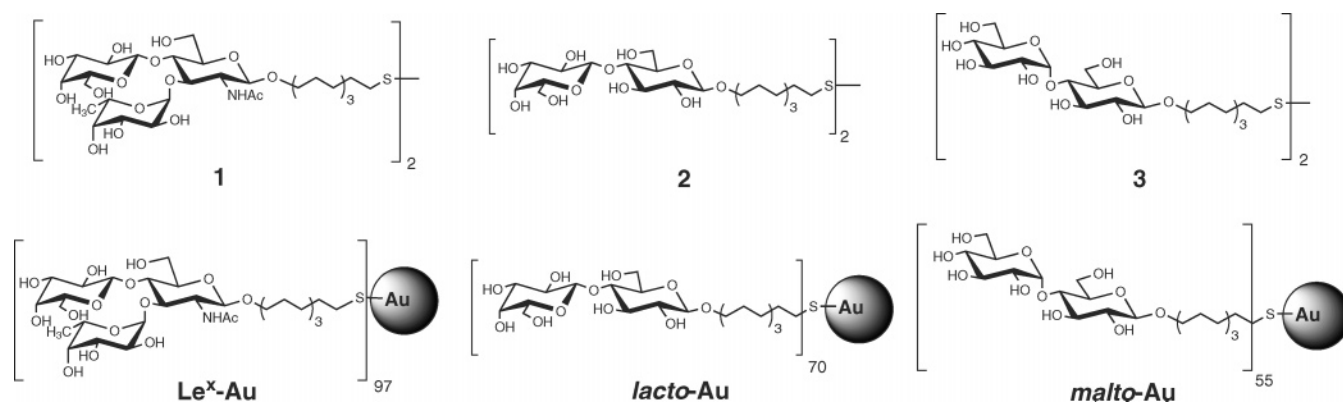(16) Zhu, T.; Zhang, X.; Wang, J.; Fu, X. Y.; Liu, Z. F. *Thin Solid Films* **1998**, *327*, 595−598.

Figure 1. Neoglycoconjugates of Le^X (**1**), lactose (**2**), and maltose (**3**) and the corresponding gold glyconanoparticles Le^X−Au, *lacto*-Au, and *malto*-Au.

membrane filter (MICROCON 30 000 Mw cutoff, 10 000*g*). This was followed by washing with water and by centrifugal filtering (six times) to remove the excess of nonbound salts, which would otherwise interfere with the AFM imaging. It is worth noting that the same centrifugal filtering process was used as part of the synthesis of the nanoparticles to purify the product, and therefore no size selection occurred via loss of small nanoparticles during preparation of the samples for AFM analysis.[10b] This was confirmed by TEM analysis of the filtrate.

Results and Discussion

Neoglycoconjugates **1**, **2**, and **3** of the trisaccharide Lewis X (Le^X) and the disaccharides lactose (*lacto*) and maltose (*malto*), and the corresponding polyvalent gold glyconanoparticles Le^X−Au, *lacto*-Au, and *malto*-Au (Figure 1), were synthesized and characterized as previously described.[10a,12] Le^X−Au GNPs, containing an average number of 97 Le^X molecules per nanoparticle, were our model system to mimic cell−cell adhesion via carbohydrate−carbohydrate interactions. The *lacto*-Au and *malto*-Au glyconanoparticles, with an average number of 70 and 55 lactose and maltose molecules, respectively, were the controls to confirm the selectivity of the Ca^{2+}-mediated Le^X−Au self-aggregation in solution.

lacto-Au GNPs were tested as control to evaluate the contribution of the lactose disaccharide in carbohydrate−carbohydrate association. Lactose is the common disaccharide of all GSLs, and its contribution to biological interaction cannot be excluded. *malto*-Au GNPs should be considered as the negative control.

Calorimetric titrations were carried out for the system formed by the GNPs and 10 mM solutions of different cations (Ca^{2+}, Mg^{2+}, or Na$^+$). The microcalorimetry curves are represented as a function of time in Figure 2. A slow aggregation process with a favorable enthalpy term of around −160 ± 30 kcal mol^{-1} per mole of GNP injected (average of seven injections; $n = 7$) was observed when Le^X−Au glyconanoparticles were added to a 10 mM calcium chloride solution (Figure 2Aii). The heat emission observed when Le^X−Au GNPs were added to a magnesium chloride solution was more than 5 times lower ($\Delta H_{app} = -30 \pm 20$ kcal mol^{-1}; $n = 4$) than in the case of calcium chloride (Figure 2B). A similar result was obtained ($\Delta H_{app} = -50 \pm 30$ kcal mol^{-1}; $n = 2$) when Le^X−Au was added to a sodium chloride solution (Figure 2C), indicating the Ca^{2+}-mediated selectivity of the Le^X aggregation. The aggregation process needed more than 1 h after each injection to reach the equilibrium. As indicated in the Experimental Section, the number of injections per run was limited by the size of the

calorimeter acquisition data files due to the slowness of Le^X−Au dilution/association underlying events.

The heat evolved upon addition of *lacto*-Au or *malto*-Au GNPs to a calcium solution (Figure 2D) was rather low, and thermal equilibrium was quickly achieved. It is worth noting that the thermal signal in the case of *lacto*-Au increases after the 4−7 first injections, suggesting that some interparticle interactions could take place as the GNPs concentration increases by successive injections of *lacto*-Au in the Ca^{2+} solution. This behavior was not observed in the case of the *malto*-Au GNPs. The results obtained clearly reveal the different thermodynamic behavior of the Le^X, *lacto*, and *malto* GNPs and demonstrate the selectivity of the Ca^{2+}-mediated self-aggregation of the Le^X−Au GNPs in aqueous solution.

The selectivity of the aggregation process of Le^X−Au GNPs was also demonstrated by AFM. At least six images were recorded for each type of GNP under each condition. Representative images are shown in Figure 3 for each type of nanoparticle before (left) and after (center) salt treatment with CaCl$_2$. Before salt treatment, the images are very similar (Figure 3, left). The estimated average particle heights for the Le^X−Au and *lacto*-Au GNPs appear very similar (2.7 ± 0.7 nm, the resolution of the instrument is estimated as 1−2 Å), and both are larger than *malto*-Au (2.0 ± 0.9) GNPs. These values match the trend in the results obtained by TEM,[10b] although the heights are rather larger than the particle diameters observed by TEM (1.8 and 1.6, respectively). This is presumably because TEM only images the gold core. However, AFM sizes (2.7 and 2.0 nm) do not match the measured gold core sizes plus the expected length of the neoglycoconjugates (3 nm). This suggests that the GNPs did not have all attached molecules in an extended configuration in air. This may have been due to the affinity of the carbohydrate molecules for the mica surface leading to a more flattened topography of the GNPs.

The auto-aggregation of the Le^X−Au, *lacto*-Au, and *malto*-Au was studied by incubating the GNPs in 10 mM calcium, magnesium, or sodium chloride solutions for 24 h, followed by washing and drying. After incubation with Ca^{2+} cations, Le^X−Au GNPs developed very large aggregates (Figure 3A, center column). The size of the aggregate shown is approximately 700 nm of diameter, but a broad range of aggregate diameters was observed. Although this aggregate is much larger that those obtained previously by TEM[10b] at similar concentration, the results obtained with both techniques agree qualitatively. In the case of the *lacto*-Au GNPs, some aggregation occurred, limited
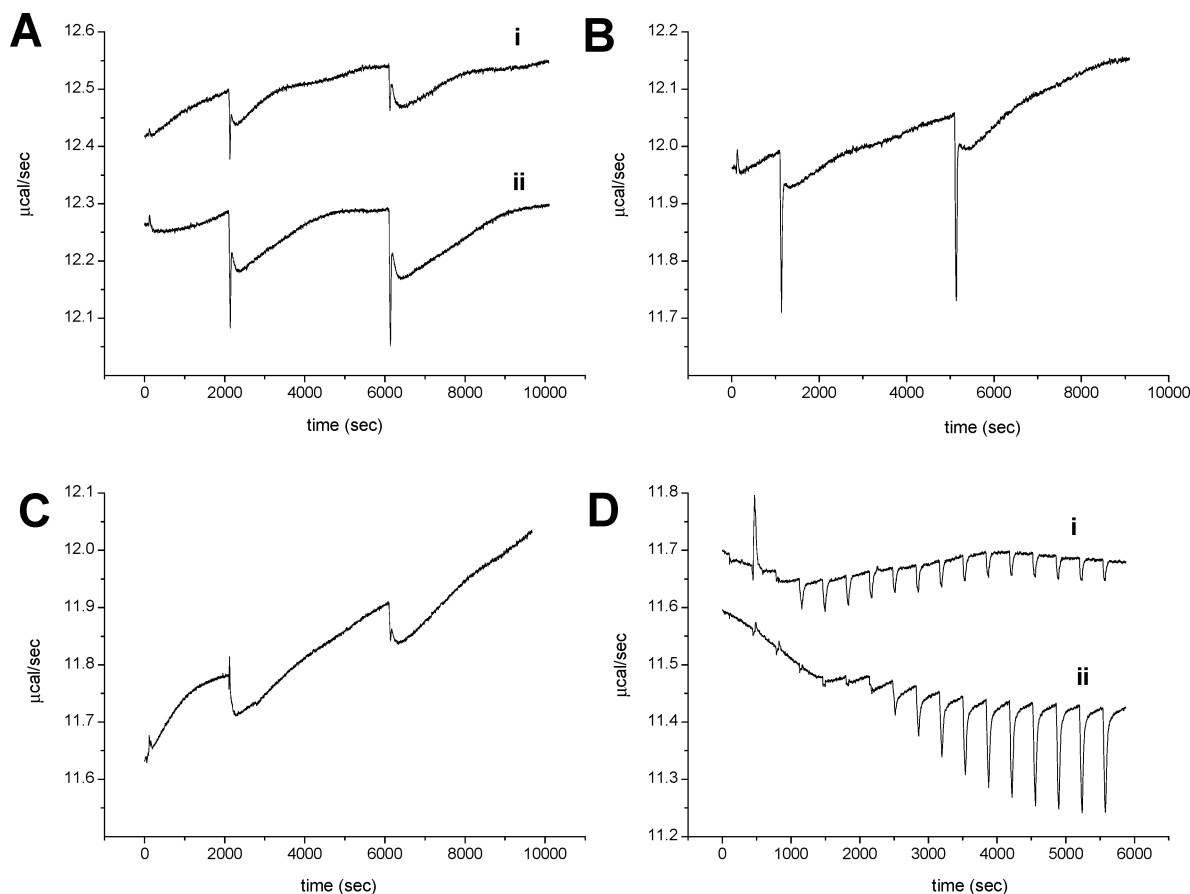
Figure 2. ITC curves for Le^X−Au added to: (A) (i) water and (ii) 10 mM CaCl$_2$; (B) 10 mM MgCl$_2$; (C) 10 mM NaCl; (D) ITC curves for *malto*-Au (i) and *lacto*-Au (ii) added to 10 mM CaCl$_2$. 15 μL injections of 50 μM GNPs were added after a first injection of 1 μL.

apparently to a few nanoparticles (Figure 3B). The largest aggregates observed for *lacto*-Au GNPs measure approximately 100 nm in diameter, and no larger aggregates such as that for Le^X nanoparticles could be observed. This observation agrees with the result observed in calorimetry, suggesting that some interparticle interaction takes place in the *lacto* GNPs in the presence of Ca^{2+}. Lactose and the trisaccharide Le^X built up the carbohydrate moiety of the Le^X GSL, and its contribution to the biological interaction cannot be excluded. The images obtained for the *malto*-Au GNPs did not show aggregation at all after incubation with Ca^{2+} (Figure 3C, center column).

In the presence of Mg^{2+}, Le^X GNPs showed some limited aggregation. However, no large aggregates such as those observed with Ca^{2+} could be detected (Figure 3A, right column). There was no definitive evidence of aggregation with either lactose or maltose GNPs in the presence of Mg^{2+} (Figure 3B and C, right column). Treatment of Le^X, *lacto*, or *malto* GNPs with 10 mM NaCl solution did not result in any aggregation, and the GNPs appeared dispersed over all of the observed surface (data not shown). These results clearly show that Ca^{2+}-mediated self-aggregation of Le^X−Au nanoparticles can be observed independently of the measurement technique or the deposition substrate (here, mica versus amorphous carbon in TEM[10b]), further reinforcing that the aggregates also form in solution. Both calorimetry and AFM results indicate that specific self-recognition events between Le^X molecules in the presence of Ca^{2+} ions dictate the aggregation process.

The calorimetric results obtained for the Ca^{2+}-mediated aggregation of Le^X GNPs clearly indicate that this association is an enthalpically favorable process ($\Delta H \approx -160 \pm 30$ kcal per mole of GNP), even though calorimetric evidence suggests that carbohydrate association in water is an unfavorable process (the excess enthalpies of mono-and oligosaccharide aqueous solutions are positive).[17] In our previous studies on carbohydrate−carbohydrate interactions using different model systems and techniques, a free energy change (ΔG) of binding ranging from -3.0 kcal mol^{-1} in the monovalent glycophane system[8b] to -8.5 kcal mol^{-1} in the polyvalent system[10d] was measured. However, in all of these systems, the association of saccharide molecules was assisted either by the presence of additional aromatic−aromatic interactions[8b] or by the immobilization on a surface of one (SPR)[10d] or two of the carbohydrate partners (AFM).[10c] The Ca^{2+}-mediated Le^X−Au self-aggregation at 25 °C proceeds with a favorable decrease of the enthalpy ($\Delta H \approx -160$ kcal mol^{-1}) and probably with an unfavorable decrease of the entropy, as it may be inferred from the free energy of binding ($\Delta G = -8.5$ kcal mol^{-1}) obtained by SPR measurements for the interaction of Le^X GNPs with Le^X SAMs.[10d]

In the Ca^{2+}-mediated aggregation of Le^X−Au, a cooperative behavior may promote the association. That is, the aggregation of the first two GNPs leads to a structure in which the next added GNP can be further stabilized by multiple interactions with the neighboring GNPs. This cooperativity may explain the average high favorable enthalpy term observed for the aggregation of Le^X GNPs in water. The molecular basis of Le^X−Le^X

(17) (a) Barone, G.; Cacace, P.; Castronuovo, G.; Elia, V.; Lepore, U. *Carbohydr. Res.* **1983**, *115*, 15−22. (b) Barone, G.; Castronuovo, G.; Elia, V.; Savino, V. *J. Solution Chem.* **1984**, *13*, 209−219.
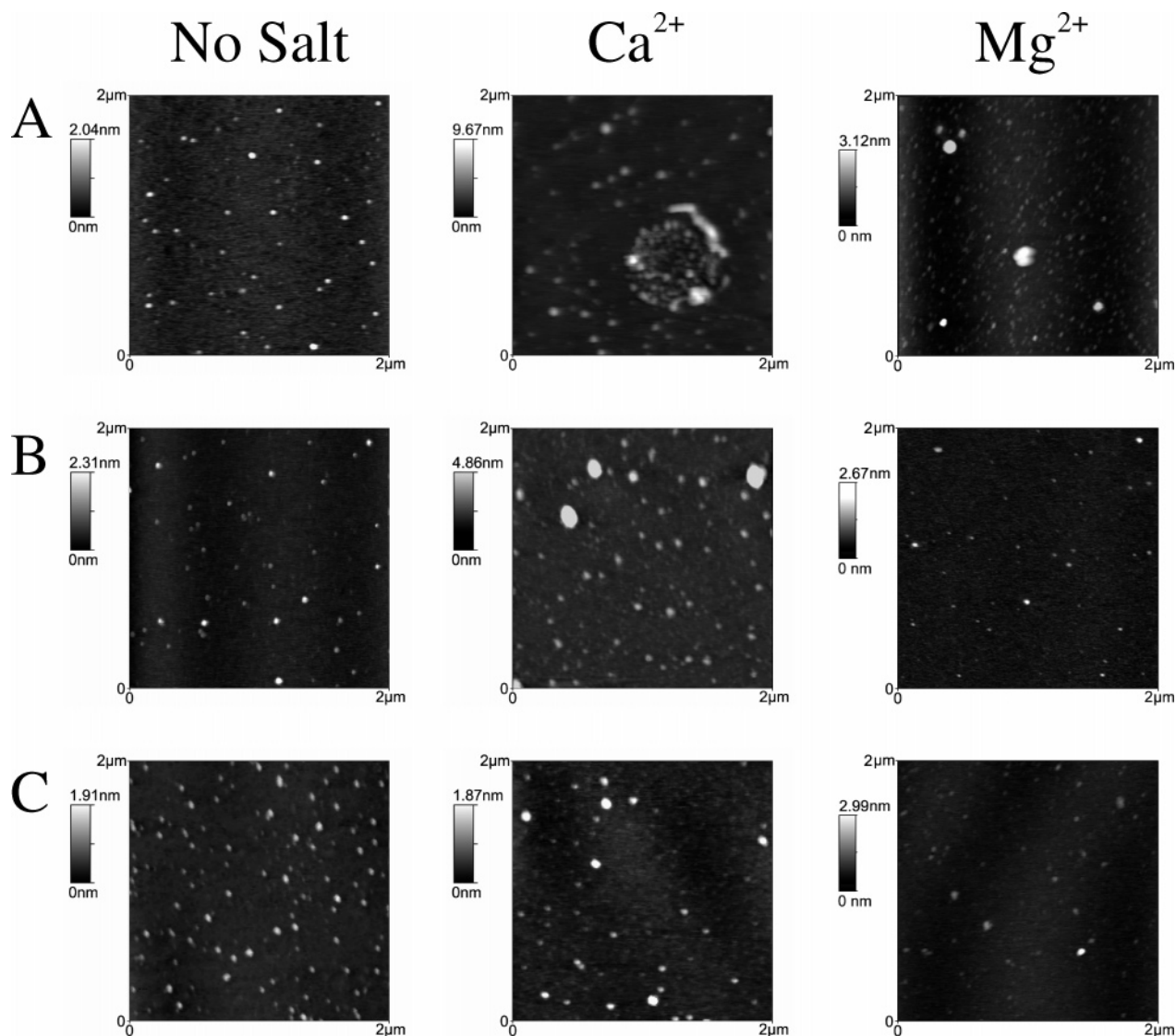
Figure 3. Noncontact AFM images of (A) Le^X−Au, (B) *lacto*-Au, and (C) *malto*-Au GNPs before (left column) and after incubation with 10 mM CaCl$_2$ solution (center column), and 10 mM MgCl$_2$ solution (right column). The bars show the height scale of the images.

interactions is not well established. However, it has been proposed that interactions between two lipophilic complementary surfaces and subsequent cross linking of two Le^X molecules via coordination of a calcium cations by four oxygen could be a mechanism that stabilizes the interaction.[18] Alternatively, the coordination of calcium cations may be the necessary first step to bring together complementary surfaces of the oligosaccharide in a suitable conformation to establish the interaction. Polyvalent presentation of the oligosaccharide seems, in any case, mandatory to stabilize and to observe the self-recognition process in water. Previous attempts to demonstrate the self-association of monomeric Le^X antigen molecules have failed.[18,19]

The present study provides the first thermodynamic evidence and visualization for the selective Ca^{2+}-mediated self-aggregation in solution of Le^X oligosaccharides in a *trans*-configuration, as was previously observed by TEM on a surface.[10b] Interaction between complementary surfaces and coordination of oxygen atoms by calcium cations probably dictate the binding events

of this enthalpy-driven process in aqueous solution. The results herein described confirm the trisaccharide Le^X as a homophilic adhesion molecule, which may be able to bring together cells in a specific configuration. Previously, we determined by AFM that the adhesion force between two Le^X antigen molecules was around 20 pN.[10c] This magnitude, although small, is significant taking into account that the adhesion force between the proteoglycan involved in the species-specific cell aggregation of the *Microciona prolifera* sponge, measured also by AFM, was found to be 40 pN.[9a] This further means that only five pairs of Le^X molecules would be enough to provide the binding strength (100 pN) between neural retina cells of embryonic chicken,[20] or that the adhesion force between 16 pairs of Le^X (320 pN) would be sufficient to hold T and B lymphocyte cells together in the absence of antigen stimulation.[21]

The extremely slow aggregation process (see Figure 2; more than 1 h to reach equilibrium) observed for the Le^X nanoparticles in the presence of calcium cations may be compared either to

(18) Kojima, N.; Fenderson, B. A.; Stroud, M. R.; Goldberg, R. I.; Habermann, R.; Toyokuni, T.; Hakomori, S. *Glycoconjugate J.* **1994**, *11*, 238−248.
(19) Wormald, M. R.; Edge, C. J.; Dwek, R. A. *Biochem. Biophys. Res. Commun.* **1991**, *180*, 1214−1221.
(20) McClay, D. R.; Wessel, G. M.; Marchase, R. B. *Proc. Natl. Acad. Sci. U.S.A.* **1981**, *78*, 4975−4979.
(21) Amblard, F.; Auffray, C.; Sekaly, R.; Fischer, A. *Proc. Natl. Acad. Sci. U.S.A.* **1994**, *91*, 3628−3632.

the Mg^{2+}-induced isodesmic self-association process of the FtsZ bacterial protein[22] or to a nucleation-elongation process, which are known to be the mechanism of, for example, actin[23] and flagellin[24] polymerization. These processes are commonly used in nature as a means to assemble in a dynamic fashion. This mechanism process requires the existence of multiple noncovalent interactions and the presence of divalent cations as is the case of Le^{X}−Au self-aggregation. Therefore, the aggregation of gold glyconanoparticles presenting Le^{X} epitopes may represent a synthetic model for mimicking dynamic association processes via carbohydrate−carbohydrate interactions. The

particular features of this interaction (e.g., low affinity, reversibility, existence of repulsive and attractive interactions) provide a reliable mechanism for a dynamic self-assembly process. Indeed, in nature the possibility of creating multiple low-energy interactions would facilitate the necessary association/dissociation events for cell adhesion and function before the onset of more stable cell−cell interactions and transduction signaling.

(22) Rivas, G.; López, A.; Mingorance, J.; Ferrándiz, M. J.; Zorrilla, S.; Minton, A. P.; Vicente, M.; Andrew, J. M. *J. Biol. Chem.* **2000**, *275*, 11740−11749.
(23) Frieden, C. *Proc. Natl. Acad. Sci. U.S.A.* **1983**, *80*, 6513−6517.
(24) Gerber, B. R.; Asakura, S.; Oosaba, F. *J. Mol. Biol.* **1973**, *74*, 467−487.